THE HIGH-TEMPERATURE RESPONSE OF THE *TRACE* 171 Å AND 195 Å CHANNELS

K. J. H. Phillips

National Research Council Senior Research Associate, NASA Goddard Space Flight Center, Code 612,
Greenbelt, MD 20771; phillips@stars.gsfc.nasa.gov

C. Chifor

Research Assistant, Catholic University of America, Washington, DC 20064; and NASA Goddard Space Flight Center,
Code 612, Greenbelt, MD 20771; chifor@stars.gsfc.nasa.gov

and

E. Landi

Artep, Inc., Ellicott City, MD 21042; and E. O. Hulbert Center for Space Research, United States Naval Research Laboratory,
Washington, DC 20375; landi@poppeo.nrl.navy.mil

ABSTRACT

The CHIANTI spectral code is used to estimate line and continuum intensity contributions to the *TRACE* 171 and 195 Å channels, widely used for imaging a variety of solar features and phenomena, including quiet-Sun and active region loops and solar flares. It is shown that the 171 Å channel has a high-temperature response due to continuum and Fe xx line emission, so high-temperature ($\sim$10–20 MK) features in flares, prominent in *TRACE* 195 Å images as well as in X-ray images from *Yohkoh* and *RHESSI*, are sometimes visible in images made in the 171 Å channel. Such features consist of hot loop-top emission, either confined spots or "spine" structures in loop arcades. This is illustrated with *TRACE* and X-ray flare images.

Subject headings: Sun: flares — Sun: UV radiation — Sun: X-rays, gamma rays

Online material: color figures

1. INTRODUCTION

Ultraviolet and extreme ultraviolet (EUV) images made by the *Transition Region and Coronal Explorer* (*TRACE*) over the past few years have revolutionized our understanding of structures in the solar atmosphere. The spatial resolution of $1''$ has revealed the fine structure of quiet-Sun, active region, and flare loops, and movies made from image sequences having a time cadence of a few seconds dramatically show the dynamic nature of the solar atmosphere. The *TRACE* instrument (Handy et al. 1999) consists of a Cassegrain telescope of 30 cm aperture, viewing approximately one-tenth of the solar disk at a time. It is divided into four quadrants, each quadrant having a multilayer coating on primary and secondary mirrors giving sensitivity in limited regions of the EUV and ultraviolet spectrum. Two of the quadrants are optimized for response in the spectral bands around 171 and 195 Å. Data from these bands have been extensively used to observe solar features.

For quiet-Sun loops with temperature 1–2 MK, Fe ix and Fe x lines dominate the emission in the 171 Å band, and Fe xii lines dominate the emission in the 195 Å band. The ratio of emission in the two bands thus gives temperature information. However, the wavelength response of each channel spans several angstroms between the half-power points, as can be seen from Figure 11 of Handy et al. (1999). (The response of the 171 Å band is in fact centered at about 174 Å but is called 171 Å to be compatible with the label used for the equivalent channel of the *Solar and Heliospheric Observatory* [*SOHO*] EUV Imaging Telescope [EIT].) For progressively higher temperature structures in the solar atmosphere, the wavelength response of these two channels includes other emission lines, and for flare loops with temperatures of 10–20 MK, the Fe xxiv 192.0285 Å emission line dominates the emission in the 195 Å channel. As

pointed out by Feldman et al. (1999), there is also a considerable contribution to the emission by the free-free continuum in both the 171 and 195 Å bandpasses.

The work of Feldman et al. (1999) was based on the MEKAL spectral code (Mewe et al. 1985). Version 5 of the CHIANTI atomic database and code (Dere et al. 1997; Young et al. 2003) enables more precise contributions to each of the *TRACE* emission bands to be found for likely solar conditions. This paper is concerned with the temperature response derived from CHIANTI synthetic spectra and corrects curves given by Handy et al. (1999) and the data of Feldman et al. (1999). We show that the 171 Å channel has a small response to high-temperature ($\sim$10–20 MK) emission and illustrate this with images of two flares.

2. THE TEMPERATURE RESPONSE OF THE *TRACE* 171 AND 195 Å CHANNELS

The wavelength response of the *TRACE* 171 and 195 Å channels is given by Handy et al. (1999) and is also available on the *TRACE* Web site.[1] In Figure 1 (*top panels*), the response curves $R(\lambda)$ are plotted against wavelength for each channel. Theoretical spectra from the CHIANTI code (ver. 5) are also given for a variety of temperatures from $T = 1$ to 20 MK. (We note that a similar plot has been given in recent work by S. Gburek et al. 2005, private communication.) The CHIANTI spectra were calculated with coronal abundances (Feldman & Laming 2000), for which elements with low ($\lesssim$10 eV) values of first ionization potential (FIP) have relative abundances that are enhanced compared with photospheric abundances by a factor of 4. Such elements include Fe and Ca, which produce many of the strong emission lines in the range of interest; emitting ions,

---

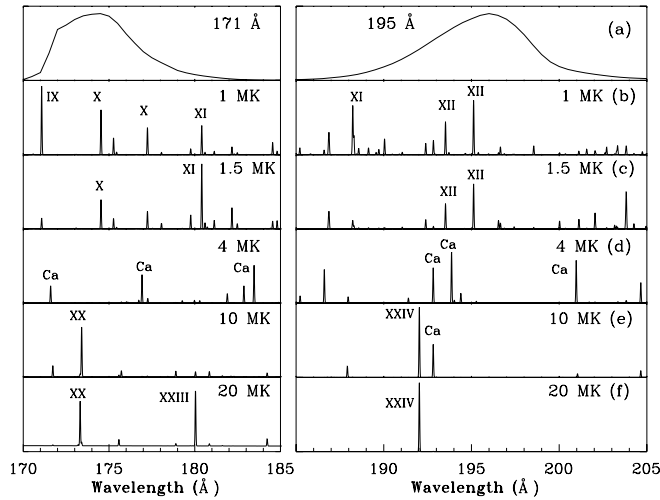[1] See http://vestige.lmsal.com/TRACE/.

Fig. 1.—Wavelength response $R(\lambda)$ in the 171 Å (*left*) and 195 Å (*right*) *TRACE* channels and CHIANTI (ver. 5) spectra for five temperatures (indicated on plots) in appropriate spectral ranges. The chief lines are identified by Roman numerals for emitting Fe ions and by "Ca" for various Ca ions. The continuum is included in each plot but is only discernible for the 171 Å spectrum at 20 MK.

wavelengths, and transitions of these lines are given in Table 1. The ionization fractions of Mazzotta et al. (1998) are also used, which for Fe are practically the same as those of Arnaud & Raymond (1992) as used in the analysis of Feldman et al. (1999). Line widths (FWHM) equal to the thermal Doppler values were used for the theoretical spectra, typical values (FWHM) being 0.017 Å for Fe x (174.5340 Å) at $T = 1$ MK; 0.023 Å for Fe XII (193.5210 Å) at $T = 1.5$ MK; and 0.081 Å for Fe XXIV (192.0285 Å) at $T = 20$ MK.

We estimated the relative contributions to the emission in the 171 and 195 Å channels made by lines and continuum by taking the product of the spectral responses and contribution functions of the lines and continuum. Following the CHIANTI definition, the contribution function $G(T)$ for a line transition $j \rightarrow i$, wavelength λ_0, is

$$G(T) = 0.83 \mathrm{Ab}(X) \frac{N(X^{+z})}{N(X)} \frac{N_j(X^{+z}) A_{ji}}{N(X^{+z}) N_e}, \qquad (1)$$

where $\mathrm{Ab}(X)$ is the abundance of element X relative to hydrogen, $N(X)$ is the number density of all ions of element X, $N(X^{+z})$ is the number density of ions X^{+z}, N_e is the number density of electrons, $N_j(X^{+z})$ is the number density of ions X^{+z} in upper level j, and A_{ji} is the radiative transition probability. A

TABLE 1
PRINCIPAL LINES WITHIN THE *TRACE* 171 Å AND 195 Å WAVELENGTH RANGES

Ion (1)	λ (Å) (2)	Transition[a] (3)	$\log T_{max}$ (4)	INTENSITIES $(\log T)$[b] 6.00 (5)	6.18 (6)	6.60 (7)	7.00 (8)	7.30 (9)
		171 Å Channel						
Continuum........................				0.003	0.006	0.361	0.512	0.847
Fe IX	171.0730	$3s^2\,3p^6\,{}^1S_0$–$3s^2\,3p^5\,3d\,{}^1P_1$	5.9	0.124	0.028	...	...	...
Ca XV..................................	171.5964	$2s^2\,2p^2\,{}^3P_0$–$2s\,2p^3\,{}^3P_1$	6.6	...	...	0.175	0.006	...
Fe XX	171.7248	$2s^2\,2p^3\,{}^2P_{1/2}$–$2s\,2p^4\,{}^4P_{1/2}$	7.0	...	...	0.025	0.046	0.001
O VI	173.0798	$1s^2\,2p\,{}^2P_{3/2}$–$1s^2\,3d\,{}^2D_{5/2}$	5.5	...	...	...	...	...
Fe XX	173.4049	$2s^2\,2p^3\,{}^2D_{5/2}$–$2s\,2p^4\,{}^4P_{5/2}$	7.0	...	...	0.001	0.367	0.053
Fe X	174.5340	$3s^2\,3p^5\,{}^2P_{3/2}$–$3s^2\,3p^4\,({}^3P)\,3d\,{}^2D_{5/2}$	6.0	0.508	0.472	...	...	...
Fe X	175.2660	$3s^2\,3p^5\,{}^2P_{3/2}$–$3s^2\,3p^4\,({}^3P)\,3d\,{}^2D_{3/2}$	6.0	0.172	0.151	...	...	...
Fe X	175.4440	$3s^2\,3p^5\,{}^2P_{3/2}$–$3s^2\,3p^4\,({}^3P)\,3d\,{}^2P_{1/2}$	6.0	0.024	0.021	...	...	...
Ni XV	176.7410	$3s^2\,3p^2\,{}^3P_0$–$3s^2\,3p\,3d\,{}^3P_1$	6.4	...	0.002	0.028	...	...
Ca XV..................................	176.9260	$2s^2\,2p^2\,{}^3P_1$–$2s\,2p^3\,{}^3P_1$	6.6	...	...	0.273	0.001	...
Fe X	177.2430	$3s^2\,3p^5\,{}^2P_{3/2}$–$3s^2\,3p^4\,({}^3P)\,3d\,{}^2P_{3/2}$	6.0	0.117	0.108	0.038	...	...
Fe XXIII.............................	180.0443	$2s\,2p\,{}^3P_2$–$2p^2\,{}^3P_1$	7.1	...	...	...	0.003	0.007
Fe XI	180.4080	$3s^2\,3p^4\,{}^3P_2$–$3s^2\,3p^3\,({}^4S)\,3d\,{}^3D_3$	6.1	0.023	0.073	0.001	...	...
Ca XIV.................................	183.4600	$2s^2\,2p^3\,{}^4S_{3/2}$–$2s\,2p^4\,{}^4P_{1/2}$	6.6	...	...	0.006	...	...
		195 Å Channel						
Continuum........................				0.047	0.001	0.105	0.237	0.042
Fe VIII	185.2130	$3p^6\,3d\,{}^2D_{5/2}$–$3p^5\,3d^2\,({}^3F)\,{}^2F_{7/2}$	5.6	0.001	...	...	...	...
Ca XIV	186.6100	$2s^2\,2p^3\,{}^4S_{3/2}$–$2s\,2p^4\,{}^4P_{3/2}$	6.6	...	...	0.010	...	...
Fe XXI	187.9247	$2s^2\,2p^2\,{}^1D_2$–$2s\,2p^3\,{}^3D_1$	7.1	...	...	...	...	...
Fe XI	188.2320	$3s^2\,3p^4\,{}^3P_2$–$3s^2\,3p^3\,({}^2D)\,3d\,{}^3P_2$	6.1	0.040	0.010	...	...	...
Fe XXIV	192.0285	$1s^2\,2s\,{}^2S_{1/2}$–$1s^2\,2p\,{}^2P_{3/2}$	7.2	...	...	...	0.461	0.953
Ca XVII..............................	192.8198	$2s^2\,{}^1S_0$–$2s\,2p\,{}^1P_1$	6.8	...	...	0.216	0.278	0.005
Fe XII	193.5210	$3s^2\,3p^3\,{}^4S_{3/2}$–$3s^2\,3p^2\,({}^3P)\,3d\,{}^4P_{3/2}$	6.2	0.171	0.187	...	...	...
Ca XIV.................................	193.8660	$2s^2\,2p^3\,{}^4S_{3/2}$–$2s\,2p^4\,{}^4P_{5/2}$	6.6	...	...	0.409	...	...
Fe XII	195.1190	$3s^2\,3p^3\,{}^4S_{3/2}$–$3s^2\,3p^2\,({}^3P)\,3d\,{}^4P_{5/2}$	6.2	0.383	0.439	...	...	...
Ca XV..................................	200.9719	$2s^2\,2p^2\,{}^3P_0$–$2s\,2p^3\,{}^3D_1$	6.6	...	0.001	0.060	0.007	...

[a] Wavelengths and transition details from CHIANTI (Dere et al. 1997).
[b] Values for the listed lines are $G(T) \times TRACE$ response R as fractions of the total emission in the 171 and 195 Å bandpasses. The continuum values are $\int G_{cont}(T, \lambda) R(\lambda)\, d\lambda$, also expressed as fractions of the total emission.
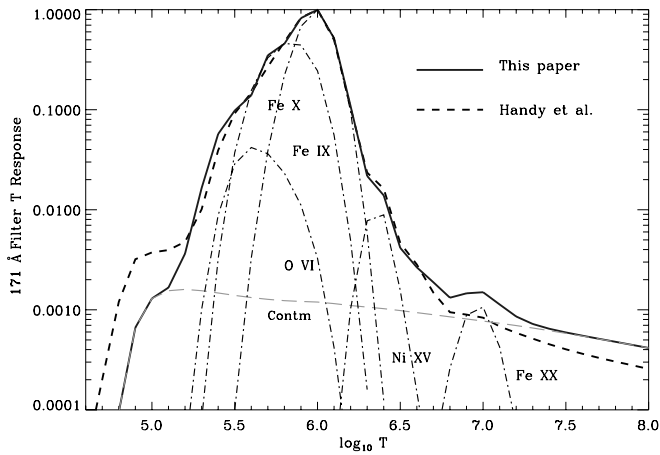
FIG. 2.—Temperature response (relative scale) of the 171 Å *TRACE* channel (*solid line*) as calculated in this work (CHIANTI ver. 5 code [Dere et al. 1997; Young et al. 2003] with Mazzotta et al. 1998 ionization fractions and Feldman & Laming 2000 coronal abundances), compared with that of Handy et al. (1999; *short-dashed line*). Also shown are $G(T)$ functions of lines emitted by ions indicated (summed if more than one line; *dot-dashed lines*) and the contribution function of the continuum (*long-dashed line*). [*See the electronic edition of the Journal for a color version of this figure.*]

FIG. 3.—Temperature response (relative scale) of the 195 Å *TRACE* channel (*solid line*) as calculated in this work, compared with that of Handy et al. (1999; *short-dashed line*). The $G(T)$ functions (*dot-dashed lines*) and continuum (*long-dashed line*) are shown (see Fig. 2). [*See the electronic edition of the Journal for a color version of this figure.*]

corresponding function for continuum (sum of free-free, free-bound, and two-photon) emission at wavelength λ, $G_{\text{cont}}(T,\lambda)$, can be defined in the same way. We note that free-free continuum is predominant at the wavelengths of interest, although there is a very small contribution from He I recombination radiation for disk flares. The contribution functions were found from the CHIANTI code. Multiplying the line $G(T)$ functions by the response $R(\lambda_0)$ in each *TRACE* channel at each line wavelength λ_0, and taking the integral $\int G_{\text{cont}}(T, \lambda)R(\lambda)\, d\lambda$ for the continuum, give the contributions to each *TRACE* channel. These are shown for some of the most intense lines and for the continuum as functions of T in Figures 2 and 3 for the 171 and 195 Å channels, respectively. In the figures, the curves for Fe X and Fe XX are the sum of the $G(T)$ functions for all lines emitted by these ions. The solid line in each figure is the sum of all line and continuum contributions and is our estimate of the temperature response of the 171 and 195 Å channels. These curves are compared with those of Handy et al. (1999), who used an earlier version of CHIANTI with coronal abundances and ion fractions from Arnaud & Raymond (1992). The main differences between our curves and those of Handy et al. (1999) in Figure 2 are the increased contribution of the Fe XX lines (in particular that at 173.4049 Å) and a higher continuum level, raising the response at $T > 20$ MK. These are due to improved atomic data (*R*-matrix instead of distorted-wave collision strengths) for Fe XX used from CHIANTI version 3 (Dere et al. 2001) and more rigorous treatment of the continuum intensities in CHIANTI version 4 (Young et al. 2003). For Figure 3, one of the main differences is the increased contribution of Fe VIII lines (e.g., at 185.2130 Å, emitted at $T < 1$ MK), owing to improved atomic data and a more complete atomic model for this ion used from CHIANTI version 3. Also, there is an increased contribution of the Ca XVII line at 192.8198 Å, owing to replacement of distorted-wave collision strengths by *R*-matrix values in CHIANTI version 4. Figure 3 shows the strong response of the *TRACE* 195 Å channel to flare (10–20 MK) temperatures, which was known from Handy et al. (1999). In addition, Figure 2 shows that there is a small response to higher temperatures through the presence of the Fe XX lines and free-free continuum in the 171 Å channel.
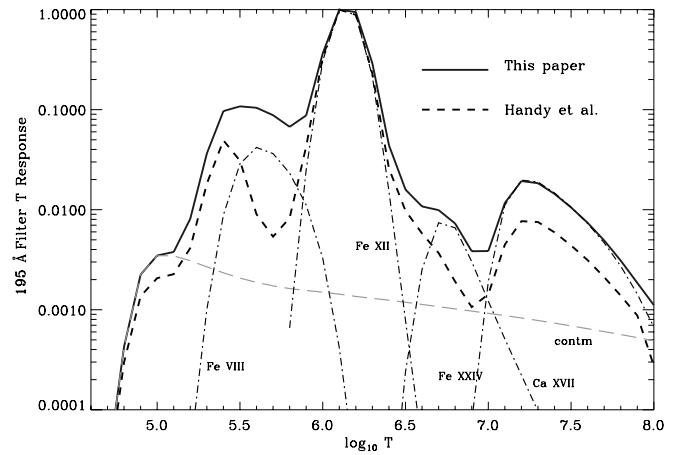
Table 1 (cols. [5]–[9]) gives contributions made by the most intense lines in each bandpass for $T = 1, 1.5, 4, 10,$ and 20 MK (i.e., for temperatures characterizing quiet, active region, and flare emission) as fractions of the total emission. At $T = 1$ MK, the Fe X 174.5340 Å and other Fe X lines are major contributors to the emission seen in the 171 Å channel; although the well-known Fe IX resonance line at 171.0730 Å is very intense, its location near the low-wavelength end of the 171 Å bandpass makes its contribution smaller than the total of all Fe X lines. At this temperature, the Fe XII 193.5210 and 195.1190 Å lines are dominant in the 195 Å channel. At $T = 1.5$ MK, Fe X lines are dominant in the 171 Å channel, and Fe XII lines are dominant in the 195 Å channel. At an active region temperature ($T = 4$ MK), the line spectrum in the range of each channel is dominated by several Ca lines, with Ca XV 171.5964 and 176.9260 Å lines important in the 171 Å channel, and Ca XVII 192.8198 Å and Ca XIV 193.8660 Å lines important in the 195 Å channel. The free-free continuum also makes a large contribution, particularly to the emission in the 171 Å channel. At $T = 10$ MK, characteristic of the decay stage of large flares, the Fe XX 173.4049 Å line is a large contributor to the 171 Å channel emission; free-free continuum emission accounts for most of the rest. In the 195 Å channel, the Fe XXIV (192.0285 Å) and Ca XVII (192.8198 Å) lines and continuum are important. For $T = 20$ MK, characteristic of the maximum phase of flares, the continuum dominates the emission in the 171 Å channel, while the Fe XXIV 192.0285 Å line accounts for almost all the emission in the 195 Å channel. The contribution of the Fe XXIV and Ca XVII lines to the emission in the 195 Å channel was pointed out by Feldman et al. (1999), but the weaker Fe XX line to the 171 Å channel at 10 MK was not; this line is near the wavelength of maximum response of the 171 Å channel emission and is therefore significant during the decay stage of flares. Feldman et al. (1999) also indicated the large contribution made by free-free continuum to the emission in both channels.

3. FLARE IMAGES FROM *TRACE* AND X-RAY INSTRUMENTS

Images of flares and postflare loops with *TRACE* are particularly instructive in showing features that have temperatures between 1 and ~20 MK. Identification of the higher-temperature features in *TRACE* images can be made with images from X-ray
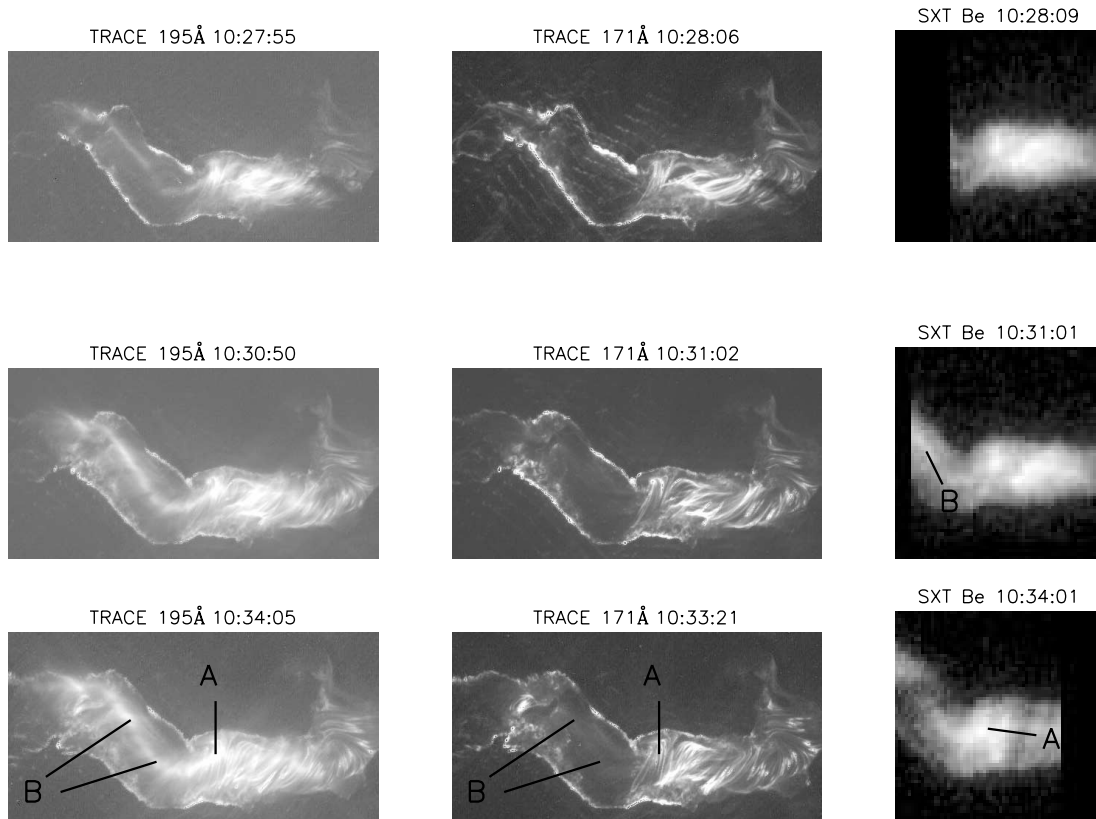
Fɪɢ. 4.—Images of the X5.7 Bastille Day flare (2000 July 14) taken in *TRACE* 195 Å (*left column*), *TRACE* 171 Å (*middle column*), and *Yohkoh* SXT (Be filter; *right column*). Times (UT) are shown above each plot. North is up in this figure; west is to the right. The flare was located at N22° W07°. The scale of the *TRACE* and SXT images is identical; the horizontal dimension of the *TRACE* images is 3.′7. "A" is the brightest location in SXT images; "B" shows the high-temperature spine structure visible in the 195 Å and SXT images, and faintly visible in the 171 Å image at 10:33:21 UT. The intensity scale for the *TRACE* images is logarithmic. [*See the electronic edition of the Journal for a color version of this figure.*]

instruments. Here, we illustrate this identification with the familiar "Bastille Day" flare, *GOES* class X5.7, on 2000 July 14, seen with *TRACE* and the soft X-ray telescope (SXT) on *Yohkoh*, and a C7.6 flare on 2003 May 28, seen with *TRACE* and the *Reuven Ramaty High-Energy Solar Spectroscopic Imager* (*RHESSI*). During the course of these two flares, there is a sequence of *TRACE* images in both the 171 and 195 Å channels with fast time cadence, so that images can be compared in the two channels.

Figure 4 shows *TRACE* 171 and 195 Å, and SXT (Be filter) images of the 2000 July 14 flare at three times, approximately 10:28, 10:31, and 10:34 UT, or 5, 8, and 11 minutes after the *GOES* X-ray maximum. Temperatures from the ratio of the two *GOES* channels indicate integrated flare temperatures at these times of 17, 17, and 15 MK, respectively. (The detectors of the *Yohkoh* Bragg Crystal Spectrometer, which are normally capable of more precise temperature information, were saturated over this period.) The SXT images were made in the Be filter, which has the highest-temperature response of all the SXT filters. The temperature response of this filter (Tsuneta et al. 1991) indicates that features visible in Be images most likely have temperatures exceeding 10 MK. The SXT images of Figure 4 were obtained nearly simultaneously with the *TRACE* images but only cover part of the field of view of the *TRACE* images. The flare occurred at N22° W07°, not far from Sun center, so the view is looking almost vertically down on the postflare loop arcade that had already formed at these times. For images at all three times, fine bright postflare loops form a prominent feature of *TRACE* 171 and 195 Å images in the western part of the loop arcade (marked "A" in Fig. 4), some almost uniform in brightness along their length, others brighter at the loop tops. Some of

these structures are visible in the SXT images, showing their high ($T \sim 15$ MK) temperatures. In the *TRACE* images, a pair of fine bright features forms the footpoints of the loops in the arcade, which separate with time. In addition, an ill-defined curved feature running along the loop arcade, approximately perpendicular to the plane of the loops and forming a "spine" structure ("B" in Fig. 4), is evident in the 195 Å images, most prominent at 10:31 UT (Fig. 4, *middle row*). This structure is also visible in SXT images, again showing its high temperature. The spine's presence in the *TRACE* 195 Å images is the result of the Fe xxɪv 192.0285 Å line in the bandpass, the $G(T)$ function that maximizes at 16 MK (log $T = 7.2$), similar to the *GOES* temperatures over this period. The spine structure is not apparent in 10:28 and 10:31 UT *TRACE* 171 Å images, although the diffraction patterns caused by the bright footpoint locations would obscure this structure if present. By 10:33:21 UT, the spine is faintly visible in 171 Å, along with another structure to the north (in the figure, these are made clearer by showing intensities on a logarithmic scale). We attribute this to the presence of a high-temperature response of the 171 Å channel due to a combination of the free-free continuum and Fe xx line emission at $T \lesssim 16$ MK. After this time, the spine structure is no longer evident in 171 Å images and much less obvious in 195 Å images. The spine is also fainter and more fragmented after 10:34 UT in SXT images. However, the spine's presence in later *TRACE* images is somewhat obscured by the formation of fine individual loop structures, which are prominent in both *TRACE* channel images but not visible in SXT images. This indicates their much lower temperatures, 1–2 MK, with emission in Fe x lines (171 Å) and Fe xɪɪ lines (195 Å). The deduction of $\sim$1 MK

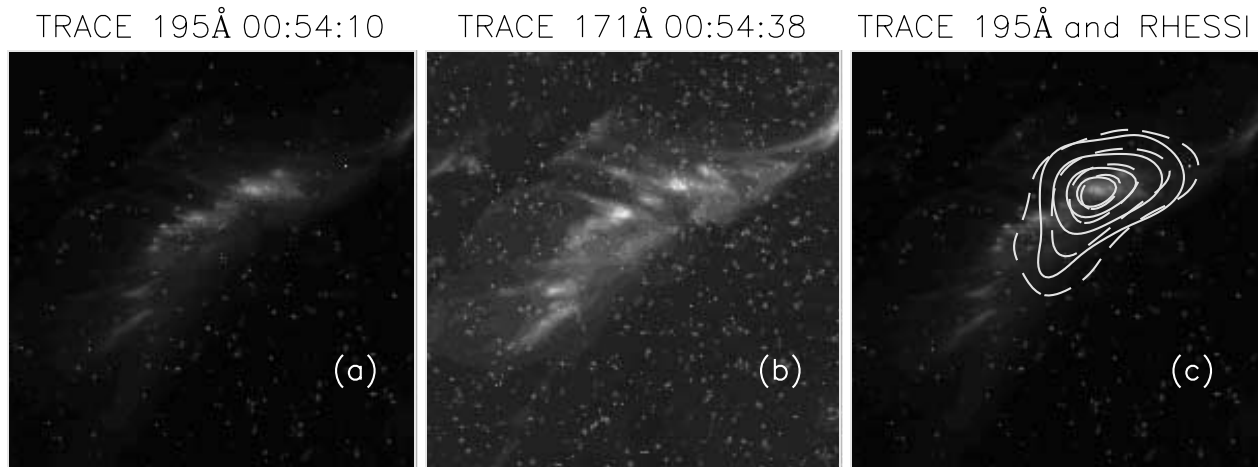TRACE 195Å 00:54:10   TRACE 171Å 00:54:38   TRACE 195Å and RHESSI

Fig. 5.—Images of the C7.6 flare on 2003 May 28 in *TRACE* (*a*) 195 Å and (*b*) 171 Å; times (UT) are indicated. North is up in this figure; west is to the right. The *TRACE* 195 Å image of panel (*a*) is shown in (*c*) with contours of emission in the 6–9 keV (*solid lines*) and 9–12 keV (*dashed lines*) X-ray range as imaged by *RHESSI* in the interval 00:54:00–00:54:28 UT. The flare was located at S05° W24°. The intensity scale for the *TRACE* images is logarithmic. [*See the electronic edition of the Journal for a color version of this figure.*]

temperatures for such loops in recent work by Patsourakos et al. (2004) is therefore correct.

Figure 5 shows *TRACE* images of the disk flare on 2003 May 28, peak *GOES* flux at 00:26 UT, with contours of X-ray emission from *RHESSI*, as a second illustration of the high-temperature response of the *TRACE* channels. This flare was located at S05° W24°, i.e., not far from Sun center, so the view is again looking down on the postflare loop system that formed after the flare onset. The *TRACE* 171 and 195 Å images (Figs. 5*a* and 5*b*) both show loop structures within the arcade, some with bright sections near their tops. One of the more prominent of these is in the northwestern part of the arcade structure. In Figure 5*c* we show the X-ray emission observed by *RHESSI* as contours, with different line styles to show the emission in the energy bands 6–9 and 9–12 keV. The image was reconstructed from modulated light curves using the `back-projection` and CLEAN algorithms in the standard *RHESSI* software package. Of the nine detectors, we used the front segments (those sensitive to X-rays as opposed to γ-rays) of detectors 4, 5, 6, 7, and 8, giving a spatial resolution of approximately $12''$. At the time, the thin attenuators (A1) were in place over the detectors to reduce excessively high photon count rates at the low-energy range of *RHESSI*; imaging and spectral analysis is therefore only possible at energies greater than $\sim$5 keV. Alignment of the *RHESSI* emission with the *TRACE* image was achieved through a comparison with the *TRACE* image and an image of the flare at 01:00 UT (i.e., 5 minutes later than the *TRACE* images) made with the *SOHO* EIT instrument. At the time of the images shown in Figure 5, the temperature obtained from single-temperature fits to the *RHESSI* thermal continuum over the range 5.3–23 keV was 22 MK. The *RHESSI* emission area is coincident with a small bright emission "knot" in the northwest part of the loop arcade in both the *TRACE* 171 and 195 Å images. As with the Bastille Day flare, the emission in the 195 Å channel can be attributed to Fe xxiv line emission, and the emission in 171 Å can be attributed to a combination of continuum and Fe xx line emission.

4. SUMMARY AND CONCLUSIONS

Using the CHIANTI (ver. 5) spectral code, we have calculated the contributions made by lines and continuum to the

emission visible in *TRACE* 171 and 195 Å images from solar features with a variety of temperatures. We confirm earlier work suggesting that Fe x and Fe xii lines are most important for quiet-Sun features with $T \sim 1$ MK, and that Fe xxiv 192.0285 Å line emission is the dominant contributor to emission in the 195 Å channel at flare temperatures. The Ca xvii 192.8198 Å line is also important for emission at $T = 4$ MK seen in the 195 Å channel. We show that the 171 Å channel also has a small response to high, flarelike temperatures, owing to contributions made by the free-free continuum and Fe xx lines, principally that at 173.4049 Å, at $T \sim 10$ MK. We also indicate that high-temperature structures in *TRACE* 171 and 195 Å images may be identified through comparison with X-ray images from the *Yohkoh* SXT for pre-2002 flares and from *RHESSI* for flares since 2002. The Bastille Day flare (on 2000 July 14) shows a remarkable instance of a "spine" structure running along the tops of loops forming an extensive arcade. This appears to be a loop-top source of the type described for more elementary flares by Feldman et al. (1994) and not simply unresolved loops. Inspection of *TRACE* images of the Bastille Day flare shows the spine to be visible very early in the flare development and its continued visibility for at least 10 minutes. If conductively coupled to the loop footpoints, the spine needs a continuing energy input with very specific spatial distribution; this might be either a complex magnetic topology such as that proposed by Jakimiec et al. (1998) or input from in-falling dark loops or "tadpole" structures, as indicated by Sheeley et al. (2004).

REFERENCES

Arnaud, M., & Raymond, J. 1992, ApJ, 398, 394
Dere, K. P., Landi, E., Del Zanna, G., & Young, P. R. 2001, ApJS, 134, 331
Dere, K. P., Landi, E., Mason, H. E., Monsignori Fossi, B. C., & Young, P. R. 1997, A&AS, 125, 149
Feldman, U., & Laming, M. 2000, Phys. Scr., 61, 222
Feldman, U., Laming, J. M., Doschek, G. A., Warren, H. P., & Golub, L. 1999, ApJ, 511, L61
Feldman, U., Phillips, K. J. H., Hiei, E., Brown, C., & Lang, J. 1994, ApJ, 421, 843
Handy, B. N., et al. 1999, Sol. Phys., 187, 229
Jakimiec, J., Tomczak, M., Falewicz, R., Phillips, K. J. H., & Fludra, A. 1998, A&A, 334, 1112

Mazzotta, P., Mazzitelli, G., Colafrancesco, S., & Vittorio, N. 1998, A&AS, 133, 403
Mewe, R., Gronenschild, E. H. B. M., & van den Oord, G. H. J. 1985, A&AS, 62, 197
Patsourakos, S., Antiochos, S. K., & Klimchuk, J. A. 2004, ApJ, 614, 1022
Sheeley, N. R., Warren, H. P., & Wang, Y.-M. 2004, ApJ, 616, 1224
Tsuneta, S., et al. 1991, Sol. Phys., 136, 37
Young, P. R., Del Zanna, G., Landi, E., Dere, K. P., Mason, H. E., & Landini, M. 2003, ApJS, 144, 135